Upper-hybrid wave-driven Alfvénic turbulence in magnetized dusty plasmas

A. P. Misra[1,*] and S. Banerjee[2]
[1]*Department of Physics, Umeå University, SE-901 87 Umeå, Sweden*
[2]*Department of Mathematics, Politecnico di Torino, 10129 Torino, Italy*
(Received 31 October 2010; revised manuscript received 8 December 2010; published 18 March 2011)

The nonlinear dynamics of coupled electrostatic upper-hybrid (UH) and Alfvén waves (AWs) is revisited in a magnetized electron-ion plasma with charged dust impurities. A pair of nonlinear equations that describe the interaction of UH wave envelopes (including the relativistic electron mass increase) and the density as well as the compressional magnetic field perturbations associated with the AWs are solved numerically to show that many coherent solitary patterns can be excited and saturated due to modulational instability of unstable UH waves. The evolution of these solitary patterns is also shown to appear in the states of spatiotemporal coherence, temporal as well as spatiotemporal chaos, due to collision and fusion among the patterns in stochastic motion. Furthermore, these spatiotemporal features are demonstrated by the analysis of wavelet power spectra. It is found that a redistribution of wave energy takes place to higher harmonic modes with small wavelengths, which, in turn, results in the onset of Alfvénic turbulence in dusty magnetoplasmas. Such a scenario can occur in the vicinity of Saturn's magnetosphere as many electrostatic solitary structures have been observed there by the Cassini spacecraft.

DOI: 10.1103/PhysRevE.83.037401 PACS number(s): 52.35.−g, 52.25.Gj, 52.25.Vy, 52.25.Xz

The nonlinear interaction of hf electrostatic upper-hybrid (UH) waves (ES-UHWs) and the lf electrostatic or electromagnetic waves in a magnetized dusty plasma is a topic of current research (see, e.g., Refs. [1–6]) as those give rise to a great variety of nonlinear effects including parametric instabilities [7], decay [8,9], as well as modulational interactions [1–6]. The latter can be responsible for the evolution of UH envelope solitons [1,3,5] and UH wave collapses [10,11], which have been observed in laboratory and space plasmas [10,12]. Moreover, the formation of such envelope solitons through the nonlinear interaction of coupled hf and lf waves is one of the most interesting features in modern plasma physics in the context of plasma turbulence [13–17], plasma heating, and particle acceleration [18]. Furthermore, the pattern formation and the existence of spatiotemporal chaos (STC) characterized by its extensive and irregular pattern dynamics in both space and time in nonlinear dynamical systems have received renewed interest (see, e.g. Refs. [13,14,16,19]).

When the electric field intensity becomes strong and approaches the modified decay instability threshold, the interaction between hf and lf waves results in "weak turbulence" in which hf waves are scattered off lf waves. However, if the electric field is so strong that it exceeds the modulational instability (MI) threshold, the interaction is then said to be in the "strong turbulence" regime, in which transfer or redistribution of wave energy to higher harmonic modes with small wavelengths can take place [13,14,16]. In this context, it is, however, believed that some sort of chaotic process may be responsible for the transfer of energy from large to small spatial scales [17].

Recently, Shukla and Stenflo [1] have developed the nonlinear theory of coupled mode interactions between ES-UHWs and modified Alfvén waves (MAWs) and predicted its application to the dusty magnetosphere of Saturn. However, they extended this work by accounting for the effects of the relativistic electron mass increase in the UH fields and the density as well as compressional magnetic field perturbations driven by the UH ponderomotive force. They made observations of a new class of oscillatory MI and spiky UH wave envelopes trapped in the electron density cavity.

On the other hand, Williams *et al.* [20] have reported observations of electric field solitary structures by the Cassini spacecraft in the vicinity of Saturn's magnetosphere with ambient magnetic fields ∼0.1–8000 nT. They also reported a range of the peak-to-peak wave amplitude by the external magnetic field as well as time durations of the solitary pulses. Moreover, it has been suggested that the turbulence in Earth's magnetosheath may account for the observations of many solitary pulses there [21]. Also, a majority of solitary structures have been found at Europa in the moon's wake, a region of known turbulence [22]. It is therefore of natural interest to investigate the possibility of the occurrence of turbulence in the vicinity of the dusty magnetosphere of Saturn, where many ES-UHWs have been observed [20]. We report here, possibly for the first time, the onset of lf Alfvénic turbulence in the nonlinear interaction of ES-UHWs and MAWs in parameter regimes that are relevant to dusty magnetospheres of Saturn. We find that redistribution of wave energy indeed takes place for higher harmonic modes, and the process becomes faster the smaller the wave number of modulation at which many unstable modes are to be excited and saturated by the MI of ES-UHWs.

In what follows, we consider the following nondimensional set of equations describing the dynamics of coupled ES-UHWs and MAWs [1]:

$$i(\partial_t + a_1\partial_x)E + a_2\partial_x^2 E + a_3(|E|^2 - N)E = 0, \quad (1)$$

$$\left(\partial_t^2 + b_1 - b_2\partial_x^2\right)N - b_3\partial_x^2|E|^2 = 0, \quad (2)$$

where the coefficients are $a_1 = 3k_0\alpha V_{Te}/\omega_H$, $a_2 = 3\alpha\omega_{pi}/2\omega_H$, $a_3 = \Omega_0^2/2\omega_H\omega_{pi}$, $b_1 = \Omega_R^2/\omega_{pi}^2$, $b_2 = V_{AR}^2/V_{Te}^2$, and $b_3 = m\mu c^2/3V_{Te}^2$, in which k_0 is the UH wave number, $\alpha = 1/(1 - 3\omega_c^2/\omega_p^2) > 0$ with $\omega_{c(p)}$ denoting the electron cyclotron (plasma) frequency, V_{Te} is the electron thermal

*apmisra@visva-bharati.ac.in

 ©2011 American Physical Society

speed, $\omega_H = \sqrt{\omega_p^2 + \omega_c^2}$ is the UH resonance frequency, and ω_{pi} is the ion plasma frequency. Also, $\Omega_0 = \sqrt{\omega_p^2 + 2\omega_c^2}$, $\Omega_R = Z_d n_{d0}\omega_{ci}/n_{e0}$ is the Rao cutoff frequency [23], $V_{AR} = \mu B_0/\sqrt{4\pi n_{i0} m_i}$ is the modified Alfvén speed [23], $\mu = n_{i0}/n_{e0}(= 1 + \delta \equiv 1 + Z_d n_{d0}/n_{e0})$ is the unperturbed ion to electron number density ratio, $m = m_e/m_i$ is the electron rest to ion mass ratio, and B_0 is the external magnetic field. Moreover, $E = E_x/E_c$ is the x component of the nondimensional UH wave electric field, with $E_c = 2m_e c\omega_p^2/\sqrt{3}e\omega_H$ and $N = n_{e1}/n_{e0}(= B_{1z}/B_0 \ll 1)$ denoting the normalized electron number density perturbation (compressional magnetic field) associated with the MAWs in dusty plasmas [5]. The space and time variables are normalized, respectively, by V_{Te}/ω_{pi} and the ion plasma period ω_{pi}^{-1}. The fourth and fifth term $\propto a_3$ in Eq. (1) arise, respectively, due to the relativistic electron mass increase and the density as well as the compressional magnetic field fluctuations that are driven by the ES-UHW ponderomotive force [for details about Eqs. (1) and (2), see, e.g., Ref. [1]].

Now, the dispersion relation for the MI of a constant amplitude UH pump of the form $E_0 \exp(ik_0 x - i\omega_H t)$+ complex conjugate can readily be obtained. Here we decompose the electric field E as the sum of the pump and its two sidebands and obtain the following dispersion law [1] (note that some terms in Ref. [1] might be missing or have been simplified somehow): $(\Omega^2 - \Omega_{AR}^2)[(\Omega - KV_g)^2 - \Delta] = 2a_3 b_3 K^2 E_0^2 \Lambda$, where $\Delta = \Lambda(\Lambda - 2a_3 E_0^2)$, $\Lambda = a_2 K^2 - a_3 E_0^2$, $\Omega_{AR}^2 = b_1 + b_2 K^2$, $V_g = a_1$ are in nondimensional forms and Ω, K are the normalized wave frequency and wave number of modulation, respectively. For the parameter values as relevant to the Saturn's magnetosphere, namely, $n_{e0} = 80$ cm^{-3}, $\delta = 10$, $T_e = 3 \times 10^7$ K, and $B_0 = 1500$ nT [20], we find that the coefficients of Ω^3 and Ω become smaller compared to the other terms. Hence the above dispersion relation can be simplified to obtain $\Omega^2 \approx \frac{1}{2}[\Omega_{AR}^2 - K^2 V_g^2 + \Delta] \pm \frac{1}{2}([\Omega_{AR}^2 + K^2 V_g^2 - \Delta]^2 + 8a_3 b_3 K^2 E_0^2 \Lambda)^{1/2}$. This shows that the ES-UHWs are modulationally unstable when the expression inside the square root becomes negative (except the case in which $\Lambda > 0$ for $K > \sqrt{a_3/a_2}E_0$ giving a purely damping mode for the lower sign) for $K < K_c$, a critical wave number. We numerically investigate some domains of K with the parameters as above for different values of the initial pump for which the MI sets in. These are, namely, $0.23 \lesssim K \lesssim 0.51$ for $E_0 = 0.2$; $0.47 \lesssim K \lesssim 0.83$ for $E_0 = 0.3$; $0.74 \lesssim K \lesssim 1.1$ for $E_0 = 0.4$; $1.1 \lesssim K \lesssim 1.4$ for $E_0 = 0.5$; and so on. In these regimes, only one solitary pattern may be formed by the master mode due to MI, and beyond this, many modes will be excited and saturated by the wave number K, as can be seen from the following simulation results.

We numerically solve Eqs. (1) and (2) using a fourth-order Runge–Kutta scheme where the spatial derivatives are approximated with centered second-order difference approximations. In the numerical scheme, we consider the time step $dt = 10^{-4}$ and assume spatial periodicity with the simulation box length $L_x = 2\pi/K$ (the resonant wavelength) together with the grid size 1024 or 2048, depending on K, so that $x = 0$ corresponds to the grid position 512 or 1024. We choose the initial conditions as [13,14,16] $E(x,0) = E_0 + E_1 \cos(Kx)$, $N = N_1 \cos(Kx)$, where $E_1 = b(b_1 + b_2 K^2)$, $N_1 = -2bb_3 E_0 K^2$, and $b = 1/500$ is an arbitrary constant to ensure that the perturbation is small. Basically, for $K_c/2 < K < K_c$, one unstable mode with spatially modulational scale $L_x = 2\pi/K$ is excited and then saturated to form a few spatially periodic solitary patterns. However, as K is lowered from $K_c/2$, there may exist many solitary patterns with spatial length scales $l_m = L_x/m$, where $m = 1$ is for the master mode and $m = 2, 3, \ldots, M$ for the unstable harmonic modes, with $M < M_p = [K_c/K]$ being due to the pattern selection. Thus the envelope E can be expressed as [13,14,16,19] $E = \sum_{m=1}^{M} E_m(t)\exp(imKx) + \sum_{m=M+1}^{\infty} E_m(t)\exp(imKx)$, in which the first summation comes from the master mode and the unstable harmonic modes, whereas the second one is due to the nonlinear interaction of hf and lf modes. We now proceed with the numerical simulation of Eqs. (1) and (2), considering $E_0 = 0.5$, for which the domain of MI for K is $1.1 \lesssim K \lesssim 1.4$. In the region $K_c/2 = 0.7 < K \lesssim 1.4$, the motion of the solitary pattern is either temporal recurrent (periodic) or pseudorecurrent (quasiperiodic), depending on the values of K.

Figure 1 shows that for $K = 1.1$, only one master pattern is formed at $x \approx 180$, implying that the system is stable. However, it can be seen from Fig. 2 that if K is lowered, that is, for $K = 0.52 < 0.7$, one master pattern and one harmonic pattern whose initial peaks are at $x \approx 750$ and 550 exhibit stochastic behaviors, which results in the coexistence of temporal chaos (TC) and spatially partial coherence (SPC). It has been shown that the resonant overlapping may be the cause for TC [19]. Furthermore, in Fig. 2, the pattern selection leads to the excitation of four solitary modes formed initially from the master mode and unstable harmonic modes. At $t \approx 45$, two solitary patterns initially peaked at $x \approx 50$ and 350 collide and fuse to form a new pattern with stronger amplitude. At the same time, strong AW emission takes place everywhere, and solitary structures are distorted. As a result, at $t \approx 90$, one solitary pattern peaked at $x \approx 550$ collides with the master pattern and gets fused into another new one. Thus, after the two collisions, there remains only one new incoherent pattern together with the distorted master pattern. However, as will be evident from the analysis of power spectra (Figs. 4–6), those

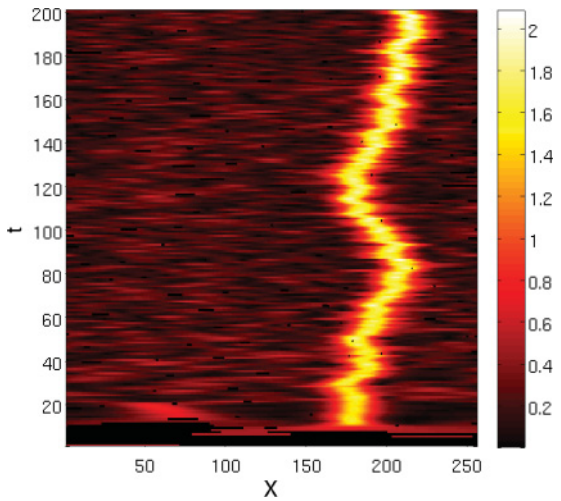

FIG. 1. (Color online) Contour of $|E(x,t)| = \text{const.}$ for $K = 1.1$ showing that the pattern selection leads to only one harmonic pattern. The system is in the coexistence of SPC and TC.

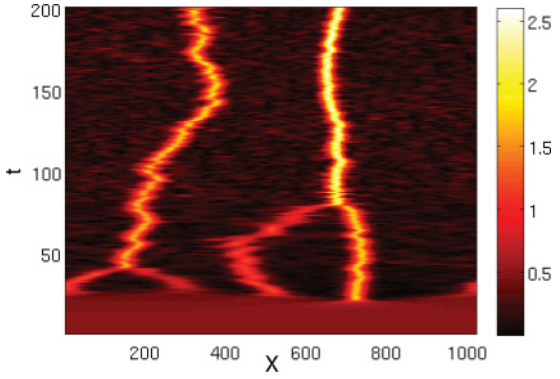

FIG. 2. (Color online) Contour of $|E(x,t)| = \text{const.}$ for $K = 0.52$. Four solitary patterns collide pairwise at $t \approx 45$ and $t \approx 90$ to fuse into two new incoherent patterns. The system is still in the coexistence of TC and STC.

few collisions are not sufficient for the cause of STC. The coherence of the system is still partially retained so that the system is in the state of TC and SPC.

Next, we consider the case in which many unstable modes are excited and saturated from the master mode, unstable harmonic modes, as well as due to nonlinear interactions to form many solitary patterns. For example, for $K = 0.1$, the pattern slection leads to 18 solitary modes (Fig. 3) in which the first collision occurs at $t \approx 45$. At longer times, only a few new incoherent patterns remain after collision and fusion among them due to strong AW emission. Four patterns initially peaked at $x \approx 1700, 1800, 1900, 2000$ collide pairwise at $t \approx 65$ and 80, respectively, to form two new patterns, which again collide with each other due to strong AW emission at $t \approx 130$ to fuse into another new pattern. Also, the harmonic pattern which was initially excited at $x \approx 1200$ disappears after some time $t \approx 110$ due to AW emission. As time goes on, several other collisions and fusions take place repeatedly. The patterns are then much distorted, and the original 18 solitary waves are finally fused into six new incoherent patterns.

We now perform a wavelet analysis of the electric field time series using a Morlet transform. Wavelets have been widely used for the analysis of time-frequency spectra in

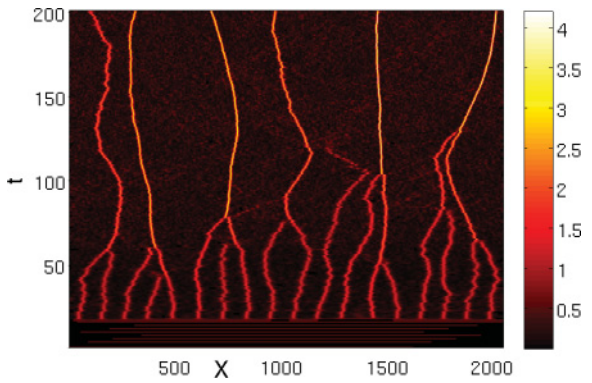

FIG. 3. (Color online) Contour of $|E(x,t)| = \text{const.}$ for $K = 0.1$. Eighteen solitary patterns, initially formed from the pattern selection, collide and fuse to form only six new incoherent patterns. The AW emission also occurs everywhere. The collision is random and not confined between two patterns. The STC state emerges.

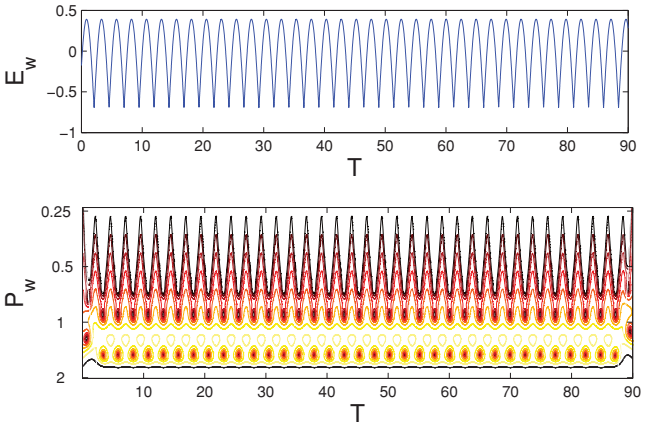

FIG. 4. (Color online) (top) The normalized wave electric field (E_w) rescaled with (bottom) the standard deviation of the sampling data and the wavelet power spectra (P_w in logarithmic scale) with respect to the sampling time T for $K = 1.1$, indicating periodic wave trains.

diverse applications, including dynamical analysis of structural systems, image processing, as well as pattern recognition in spatiotemporal systems [24]. In order to recognize the spatiotemporal features of the present system, as observed in Figs. 1–3, we analyze the corresponding data of the electric field for different values of $K = 1.1$, 0.52, and 0.1, as above. To this end, we rescale the absolute value of the electric field amplitude as (E_W) by the standard deviation of the sampling data and plot against the sampling time T (with a time step 0.01), which depends on the size of the data considered. In our analysis, we have used a Morlet wavelet as the mother wavelet, which offers a good balance between time and frequency localizations and consists of a plane wave modulated by a Gaussian wave function. The Morlet transform is then used to calculate the wavelet for the field at the significance level with variance $\sigma^2 = 1$. The corresponding wavelet power spectra of the time series shown in the upper panels of Figs. 4–6 are visualized in the lower panels of the same figures. We see that at a certain interval of T, the pattern shows a regular simple periodic train of waves for $K = 1.1$ (Fig. 4). This result is consistent with the contour plot as shown in Fig. 1. When $K = 0.52$, Fig. 5 indicates a quasiperiodic wave train, that is, chaotic in time but maybe partially periodic in space, as

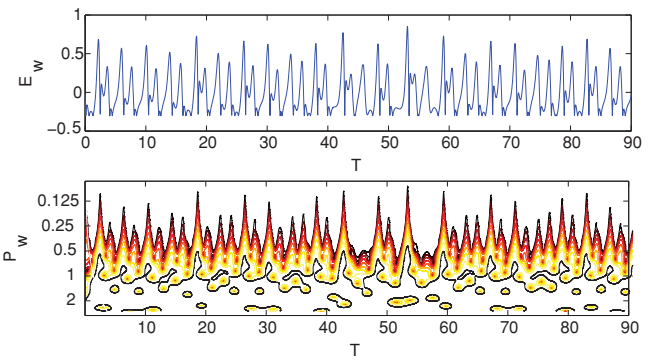

FIG. 5. (Color online) Same as in Fig. 4, but for $K = 0.52$, indicating the state of temporal chaos but spatially partial coherence.

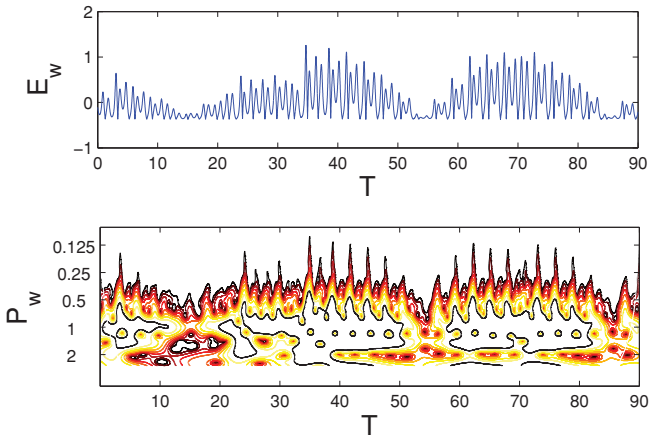

FIG. 6. (Color online) Same as in Fig. 4, but for $K = 0.1$, indicating that the motion is strongly chaotic in both space and time.

analogous to the behaviors depicted in Fig. 2. Finally, strong chaotic motion can be seen in Fig. 6 for $K = 0.1$, which agrees with the features observed in Fig. 3.

Thus, in the process of collision and fusion, strong chaotic activity in both space and time can be observed in the present system. As a result, there remains, after a longer time, few incoherent patterns together with few stable higher harmonic modes excited through nonlinear interactions. A certain amount of the system energy, which was initially confined to many solitary waves, is now redistributed into those new incoherent patterns as well as to stable higher harmonic modes with short wavelengths ($K > K_c$). The transport of the trapped electrons then occurs, and electrons can thus be accelerated across the magnetic field via a surfatron acceleration mechanism [25]. So if, initially, there exist a number of unstable modulation lengths to form many solitary patterns, pattern evolution (i.e., collision, fusion, and distortion among them) and strong AW emission can lead to the STC state and hence to the onset of turbulence in dusty magnetoplasmas. However, the mechanism that leads to the state of STC is still remains unclear.

We ought to mention that in the present investigation, we have considered the parameter regimes that give positive group dispersion ($\alpha > 0$) of the UH waves. In the opposite case, that is, for $\alpha < 0$, one needs to consider some higher magnetic field strength than that considered here. This may, however, give rise stable wave propagation [4,26]. Furthermore, the effect of the cubic nonlinear term in Eq. (1), which appears due to the relativistic electron mass increase, is to enhance the excitation of many more unstable harmonic modes and hence the faster dynamical transition from order to STC than the nonrelativistic case [2]. On the other hand, the stationary charged dust grain, which modifies the frequency of the modulated ES-UHWs and hence the associated instability growth rate, does not change the qualitative behaviors (except that the collision and fusion among the patterns somewhat differ at different times and the wave amplitude decreases slightly at a specific time) of the nonlinear interactions as shown in Fig. 3; that is, the number of modes initially excited at different modulational length scales and the number of remaining modes (i.e., six) after collision and fusion among them remain the same. Moreover, the nonlinear coupling of colliding multiple UH wave envelopes (head-on collisions) that may give rise to the stability of one-dimensional envelope solitons due to negative group dispersion ($\alpha < 0$) could be an another important investigation [26] but is beyond the scope of the present study.

It is to be mentioned that although there are no direct or indirect observations, in particular, for localized UH wave envelopes coupled with AWs, based on the recent observations, that is, the existence of many electric field solitary structures in the vicinity of Saturn's magnetosphere with the magnetic fields 0.1–8000 nT [20], and also on the fact that the equatorial plane of Saturn contains charged dusts, and dusty plasma can move across the magnetic field lines [2], we conclude that the present results could give insight for understanding the origin of lf Alfvénic turbulence that can occur in Saturn's magnetosphere. However, as of 2010, the magnetosphere of Saturn still remains an important subject of ongoing investigation by the Cassini mission.

A.P.M. acknowledges support from the Kempe Foundations, Sweden, through Grant No. SMK-2647.

[1] P. K. Shukla and L. Stenflo, J. Plasma Phys. **73**, 3 (2007).
[2] P. K. Shukla *et al.*, Phys. Plasmas **10**, 4572 (2003).
[3] B. Eliasson *et al.*, Phys. Plasmas **10**, 3539 (2003).
[4] A. N. Kauffman and L. Stenflo, Phys. Scr. **11**, 269 (1975).
[5] P. K. Shukla *et al.*, Phys. Rep. **138**, 1 (1986).
[6] H. Pcseli, IEEE Trans. Plasma Sci. **13**, 53 (1985).
[7] M. Porkolab *et al.*, Phys. Fluids **19**, 872 (1976).
[8] L. Stenflo *et al.*, Planet. Space Sci. **40**, 473 (1992).
[9] S. Goodman *et al.*, Phys. Plasmas **1**, 1765 (1994).
[10] P. J. Christiansen, V. K. Jain, and L. Stenflo, Phys. Rev. Lett. **46**, 1333 (1981).
[11] L. Stenflo, Phys. Rev. Lett. **48**, 1441 (1982).
[12] B. Grek and P. K. Shukla, Phys. Rev. Lett. **30**, 836 (1973).
[13] A. P. Misra *et al.*, Phys. Rev. E **79**, 056401 (2009).
[14] S. Banerjee, A. P. Misra, P. K. Shukla, and L. Rondoni, Phys. Rev. E **81**, 046405 (2010).
[15] A. P. Misra *et al.*, Phys. Plasmas **17**, 032307 (2010).
[16] X. T. He, C. Y. Zheng, and S. P. Zhu, Phys. Rev. E **66**, 037201 (2002).
[17] F. B. Rizzato, G. I. deOliveira, and R. Erichsen, Phys. Rev. E **57**, 2776 (1998).
[18] D. Eichler, Astrophys. J. **224**, 1038 (1978).
[19] X. T. He and C. Y. Zheng, Phys. Rev. Lett. **74**, 78 (1995).
[20] J. D. Williams *et al.*, Geophys. Res. Lett. **33**, L06103 (2006).
[21] J. S. Pickett *et al.*, Ann. Geophys. **22**, 2515 (2004).
[22] W. S. Kurth *et al.*, Planet. Space Sci. **49**, 345 (2001).
[23] N. N. Rao, J. Plasma Phys. **53**, 317 (1995).
[24] G. Hangshan *et al.*, Appl. Math. Mech. **19**, 593 (1998).
[25] T. Katsouleas and J. M. Dawson, Phys. Rev. Lett. **51**, 392 (1983).
[26] P. K. Shukla *et al.*, Phys. Lett. A **313**, 424 (2003).